SUPPLEMENTAL MATERIAL

Table S1. Molecular categories among patients with IDH mutations in TCGA, related to Figure 4.

	Number of patients (% in TCGA)
Oligodendroglioma + 1p/19q codeletion	127 (11.5%)
Astrocytoma without CDKN2A/2B HD (Grade 2-3)	123 (11.1%)
Astrocytoma with CDKN2A/2B HD (Grade 2-3)	11 (0.98%)
Astrocytoma Grade 4	25 (2.3%)

Table S2. CHARM predicted the characteristic genetic alterations listed in the *2021 WHO Classification of Tumors of the Central Nervous System*, related to Figure 5. A summary of the model performance is shown.

	Lower-Grade Histology			Grade 4 Histology		
	CNN	CHARM	Ref [1]	CNN	CHARM	Ref [1]
ATRX Mutation	0.79 ± 0.055	0.79 ± 0.052	0.77	0.67 ± 0.117	0.68 ± 0.065	N/A
TP53 Mutation	0.81 ± 0.05	0.87 ± 0.041	0.83	0.62 ± 0.061	0.70 ± 0.047	0.66
CDKN2A/B Homozygous Deletion	0.7 ± 0.078	0.80 ± 0.063	0.64	*N/A		N/A
CIC Mutation	0.76 ± 0.048	0.79 ± 0.03	0.76		N/A	
1p 19q codeletion	0.74 ± 0.021	0.82 ± 0.047	N/A		N/A	
7 gained and 10 lost	0.73 ± 0.049	0.76 ± 0.034	N/A	0.50 ± 0.080	0.55 ± 0.054	N/A
EGFR amplification	0.73 ± 0.113	0.77 ± 0.079	0.69	0.64 ± 0.044	0.71 ± 0.031	0.737

*Fewer than 10 patients with these genetic alterations.

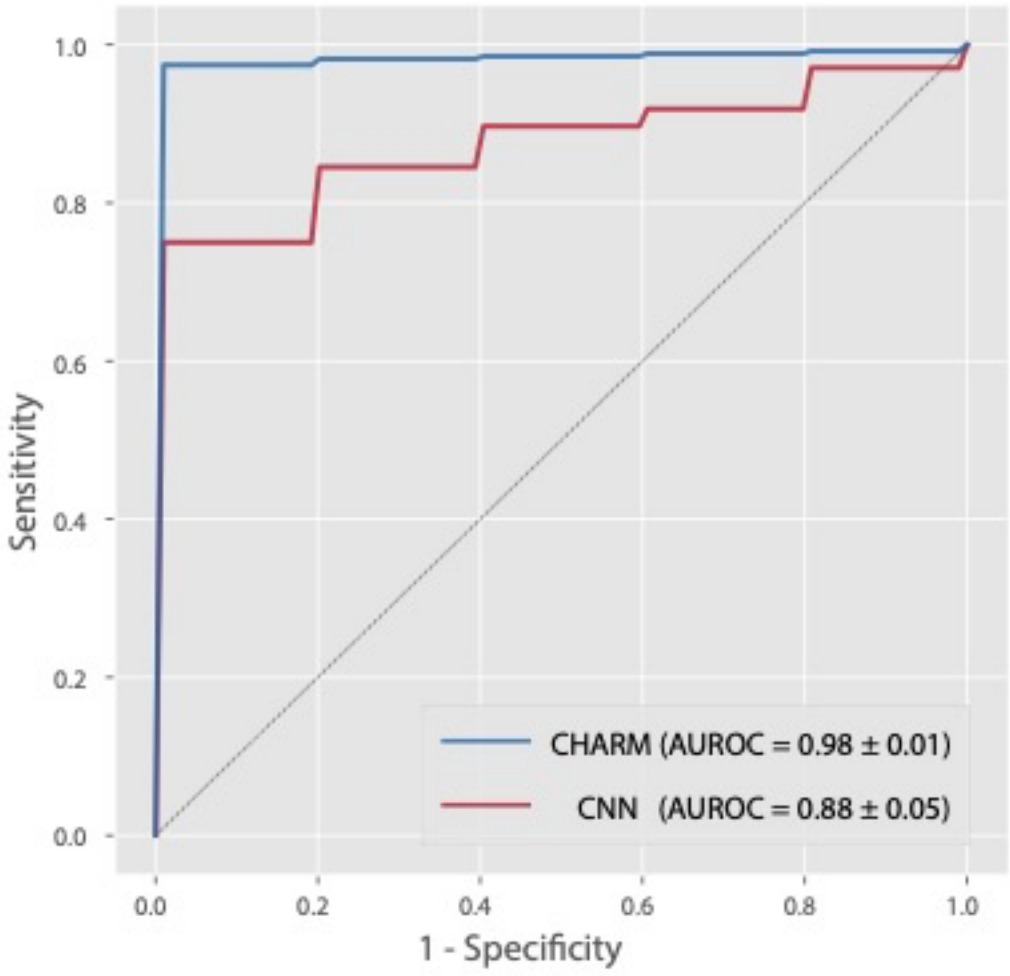

Figure S1. CHARM identified cryosections with malignant tissues on the independent validation dataset, related to Figure 2. We evaluated the generalizability of CHARM on the independent validation dataset. The AUROC of CHARM is 0.98 ± 0.01, which is significantly higher than that of the CNN-based model (AUROC = 0.88 ± 0.05; Wilcoxon signed-rank test P = 0.04).

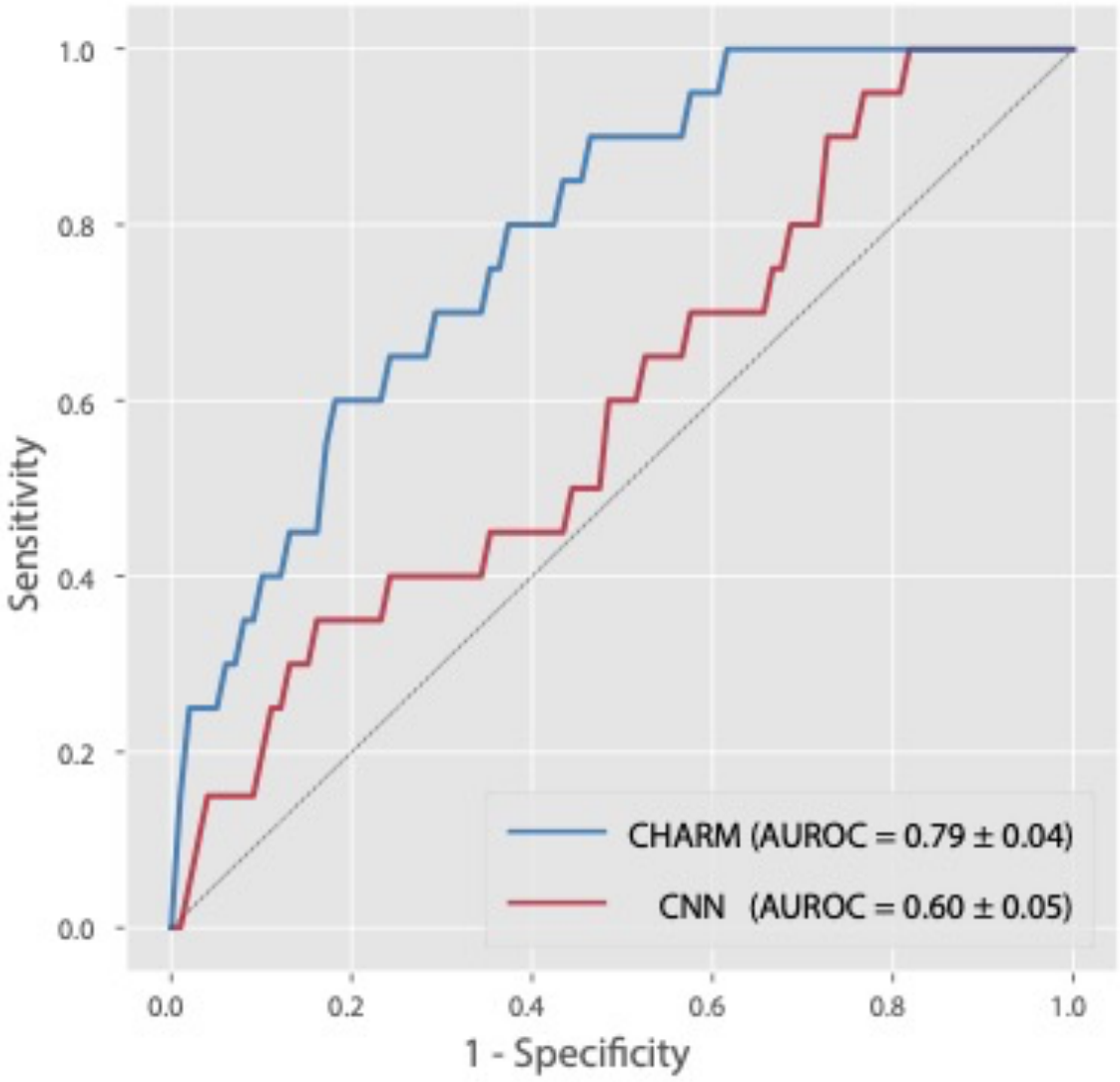

Figure S2. CHARM predicted IDH status among glioma samples with high histologic grades (AUROC = 0.79 ± 0.04), related to Figure 3. CHARM attained significantly better performance than that of the CNN-based model (AUROC = 0.60 ± 0.05, Wilcoxon signed-rank test P-value = 0.04).

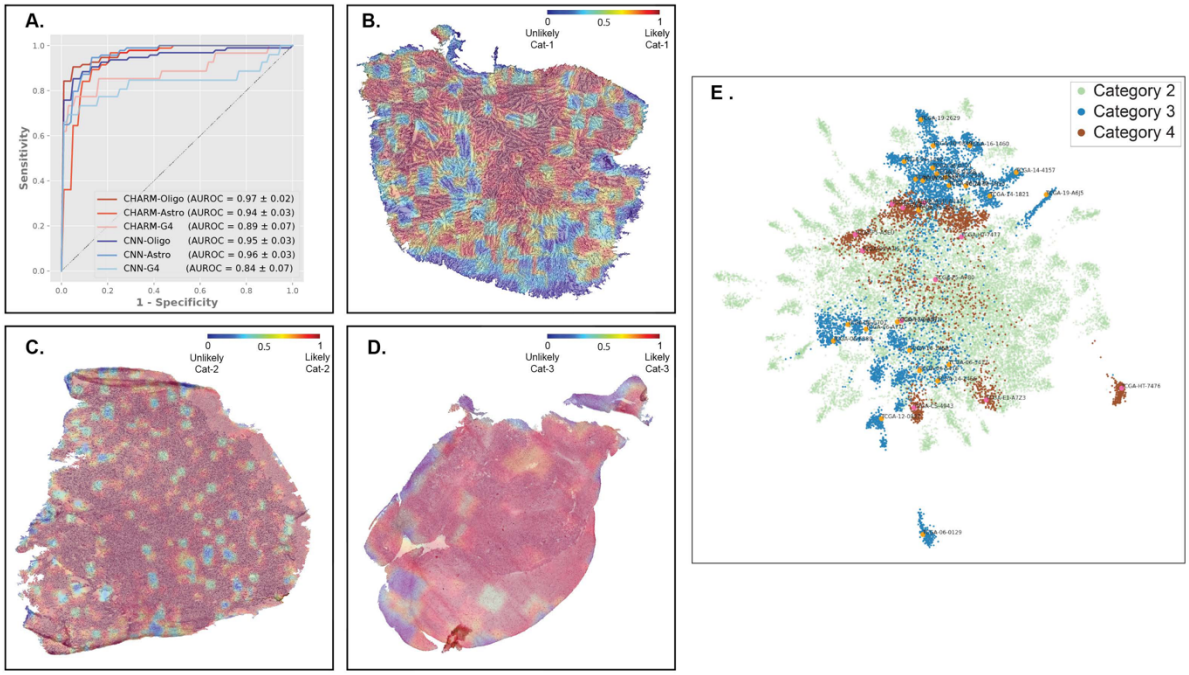

Figure S3. CHARM classified glioma subtypes defined by the *2021 WHO Classification of Tumors of the Central Nervous System*, related to Figure 4. (A) Both CHARM and CNN-based models successfully classified glioma patients based on the *2021 WHO Classification*. We focused on three prevalent types of adult gliomas: oligodendroglioma with *IDH* mutation and 1p/19q codeletion (category 1; CHARM = 0.97 ± 0.02; AUROC of CNN = 0.95 ± 0.03;), astrocytoma with *IDH* mutation but without *CDKN2A/2B* HD (category 2; CHARM: 0.94 ± 0.03; CNN: 0.96 ± 0.03), and astrocytoma with grade 4 histologic features and *IDH* mutation (category 3; CHARM: 0.89 ± 0.07; CNN: 0.84 ± 0.07). **(B)** Visualized the regions of interest identified by our machine learning models for categories 1, 2, and 3, respectively. “1” in red indicates the regions

most relevant to the corresponding glioma category. The attended regions span the homogeneous tissue, which demonstrates frozen artifact associated with edema, and a monomorphous population of cells. **(C)** Attention is distributed across the homogeneous sample, which demonstrates hypercellularity and abundant dilated vasculature. **(D)** Attention is given to the densest areas of glioma, which have cells with large, irregular, hyperchromatic nuclei, plump eosinophilic cytoplasm, and foci of incipient necrosis and microvascular proliferation. **(E)** Summarized feature spaces extracted by our machine learning models. The proximity between the clusters of “histologic grade 4” category 3 (in blue) and “molecular grade 4” category 4 (astrocytoma histology with *IDH* mutation and *CDKN2A/2B* HD, a rare subtype; in brown) glioma demonstrates the potential to discover similarities in the histopathology image features extracted by machine learning methods, which may not be apparent to pathologists.

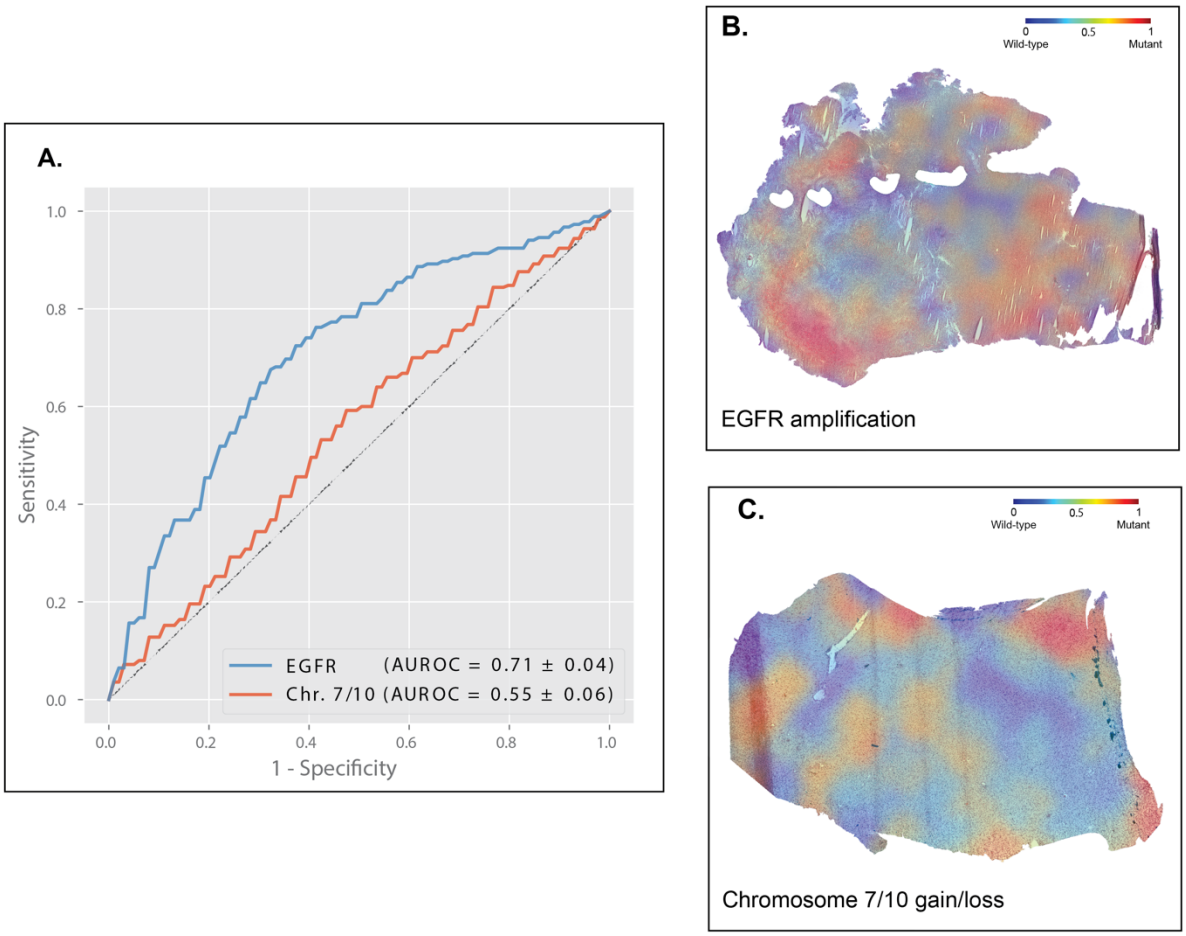

Figure S4. CHARM predicts characteristic genetic alterations listed in the 2021 WHO Classification among high-histologic-grade glioma patients, related to Figure 5. (A) CHARM identified cryosection samples with EGFR amplification with an AUROC of 0.71 ± 0.031 and predicted chromosome 7/10 gain and loss with an AUROC of 0.55 ± 0.054 among high-histologic-grade glioma samples. **(B)** The heatmap of a sample with EGFR amplification demonstrates high attention in areas of prominent vascularity, in this otherwise relatively histologically homogeneous tumor. **(C)** Attention visualization of the CHARM model for predicting chromosome 7/10 gain and loss. In the

regions receiving high attention weight, there are mild variations in cellularity, suggesting infiltration of the tumor cells into brain parenchyma. The heatmap highlights patches in all different cellularity levels.

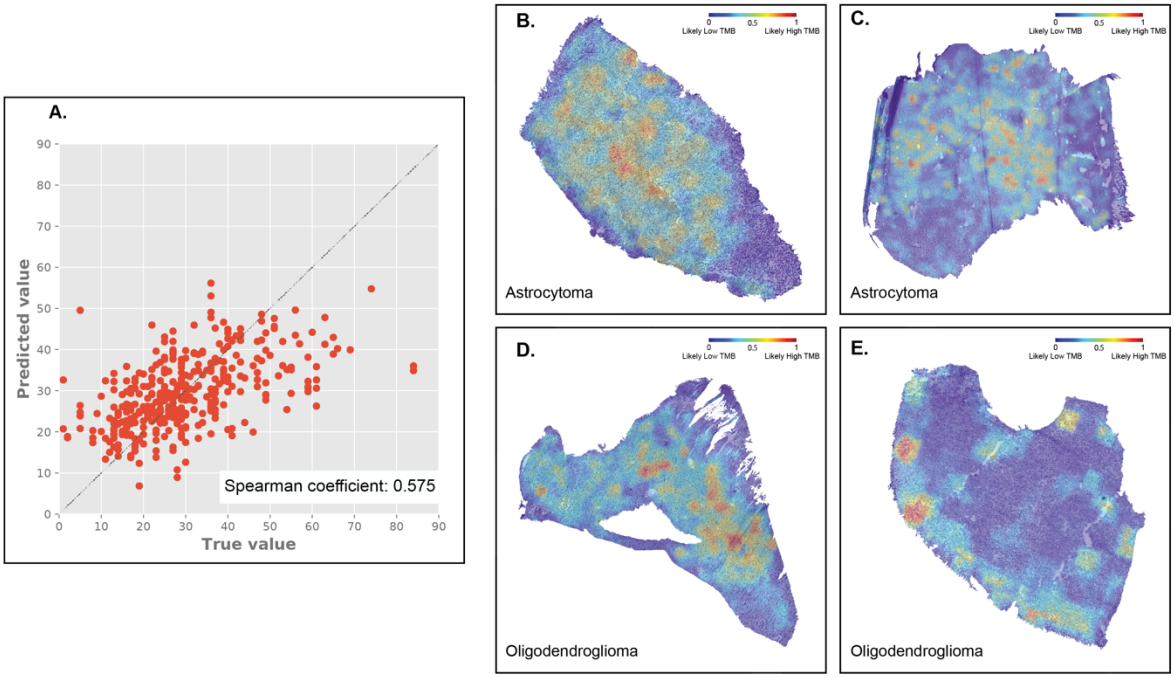

Figure S5. Deep learning models predicted the tumor mutation burden of glioma samples using cryosection histopathology images, related to Figure 5. We stratified our analyses by histologic grades to identify quantitative histopathology predictors independent of grades. **(A)** The scatter plot shows the correlations between the measured and predicted TMB values. **(B)** Our histopathology-based prediction model identified regions of interest that contribute to the prediction of TMB values in astrocytoma samples. “1” in red indicates the regions with high predicted TMB. “0” in blue indicates the regions with low predicted TMB. Patients with high TMB show greater cellularity and atypia, with attended patches highlighting less edematous regions in this representative histopathology slide. **(C)** Patients with low TMB display less dense cellularity and decreased atypia relative to high TMB cases, as represented in this slide. **(D)** Visualization of our prediction results in oligodendroglioma samples. The amount of attention paid to each region of the histopathology images is shown. For both

visualizations, “1” is for high TMB (red). Oligodendrogliomas with greater atypia, cellularity, and clear cortical infiltration are correctly predicted to have higher TMB. **(E)** Lower cellular oligodendrogliomas are correctly predicted to have lower TMB.

References

1. Fu, Y., Jung, A.W., Torne, R.V., Gonzalez, S., Vöhringer, H., Shmatko, A., Yates, L.R., Jimenez-Linan, M., Moore, L., and Gerstung, M. (2020). Pan-cancer computational histopathology reveals mutations, tumor composition and prognosis. Nat Cancer *1*, 800-810. 10.1038/s43018-020-0085-8.